



UNIVERSIDADE ESTADUAL DE CAMPINAS  
SISTEMA DE BIBLIOTECAS DA UNICAMP  
REPOSITÓRIO DA PRODUÇÃO CIENTIFICA E INTELECTUAL DA UNICAMP

**Versão do arquivo anexado / Version of attached file:**

Versão do Editor / Published Version

**Mais informações no site da editora / Further information on publisher's website:**

<https://pos.sissa.it/395/304>

**DOI: 10.22323/1.395.0304**

**Direitos autorais / Publisher's copyright statement:**

©2022 by Sissa Medialab. All rights reserved.

## Observations of the cosmic ray detector at the Argentine Marambio base in the Antarctic Peninsula

N. A. Santos <sup>a,\*</sup>, S. Dasso <sup>a,b,c</sup>, A. M. Gulisano <sup>b,c,d</sup>, O. Areso <sup>b</sup>, M. Pereira <sup>b</sup>, H.

Asorey <sup>e,f</sup> and L. Rubinstein <sup>b,g</sup> on behalf of the LAGO Collaboration

(a complete list of authors can be found at the end of the proceedings)

<sup>a</sup>Universidad de Buenos Aires (UBA), Facultad de Ciencias Exactas y Naturales (FCEN), Departamento de Ciencias de la Atmósfera y los Océanos (DCAO)

Pabellón 2 - Intendente Güiraldes 2160 - Ciudad Universitaria, Buenos Aires, Argentina.

<sup>b</sup>Consejo Nacional de Investigaciones Científicas y Técnicas (CONICET) - Universidad de Buenos Aires, Instituto de Astronomía y Física del Espacio (IAFE)

Intendente Güiraldes 2160 - Ciudad Universitaria, Buenos Aires, Argentina.

<sup>c</sup>Universidad de Buenos Aires (UBA), Facultad de Ciencias Exactas y Naturales (FCEN), Departamento de Física (DF)

Pabellón 1 - Intendente Güiraldes 2160 - Ciudad Universitaria, Buenos Aires, Argentina.

<sup>d</sup>Instituto Antártico Argentino, Dirección Nacional del Antártico

25 de mayo 1143, Buenos Aires, Argentina.

<sup>e</sup>Instituto de Tecnologías en Detección y Astropartículas (ITeDA, CNEA/CONICET/UNSAM)

Centro Atómico Constituyentes, Av. General Paz 1499, Buenos Aires, Argentina.

<sup>f</sup>Laboratorio de Acústica y Electroacústica (LACEAC), Departamento de Electrónica, Facultad de

Ingeniería, Universidad de Buenos Aires

Av. Paseo Colón 850, Buenos Aires, Argentina.

E-mail: [nsantos@at.fcen.uba.ar](mailto:nsantos@at.fcen.uba.ar), [sdasso@iafe.uba.ar](mailto:sdasso@iafe.uba.ar),

[adriangulisano@gmail.com](mailto:adriangulisano@gmail.com), [areso@iafe.uba.ar](mailto:areso@iafe.uba.ar), [matiaspereira@iafe.uba.ar](mailto:matiaspereira@iafe.uba.ar),

[hernan.asorey@iteda.cnea.gov.ar](mailto:hernan.asorey@iteda.cnea.gov.ar), [lrubinstein@iafe.uba.ar](mailto:lrubinstein@iafe.uba.ar)

In March 2019 a Space Weather Laboratory was deployed at Marambio base in the Antarctic Peninsula. The main instrument installed was a cosmic ray detector based on water Cherenkov radiation. This detector is the first permanent Antarctic node of LAGO Collaboration (Latin American Giant Observatory). LAGO Project is an extended Astroparticle Observatory and it is mainly oriented to basic research in three branches of Astroparticle physics: the Extreme Universe, Space Weather phenomena, and Atmospheric Radiation at ground level. LAGO Space Weather program is directed towards the study of how the variations of the flux of secondary cosmic rays at ground level are linked with the heliospheric and geomagnetic modulations. Observations made during 2019 and 2020 are presented here. We analyze the effect of barometric pressure and local temperature in the count rate. The corrected count rate observed with the water Cherenkov detector is compared with observations of Oulu neutron monitor which has similar rigidity cut-off than the Marambio site.

37<sup>th</sup> International Cosmic Ray Conference (ICRC 2021)

July 12th – 23rd, 2021

Online – Berlin, Germany

---

\*Presenter

## 1. Introduction

The modulation of low-energy galactic cosmic rays (CRs) intensity near Earth is controlled by solar activity. This phenomena comprises a number of effects including the eleven-year variation, quiet-time anisotropies of various sorts, and transient effects such as Forbush decreases (FDs) behind shock fronts.

Continuous monitoring of the CR anisotropies and time variabilities at individual stations is relevant for Space Weather (SW) research in the sense that they may serve as a tool for remote sensing of the conditions in the heliosphere.

The world-wide network of neutron monitors (NMs) is the standard instrument to investigate the variations of the CR flux at Earth in the  $\sim$  GeV range. However, also different detector systems are able to track the evolution of the CR intensity, for instance, muon telescopes or particle counters from high-energy experiments. The Pierre Auger collaboration showed that water Cherenkov detectors (WCDs) are highly sensitive to Forbush decreases and other transient events related to solar modulation of CRs when they are operating in the “single particle technique” mode which consists in record low-threshold rates with all the surface detectors of the array [1, 2].

The Latin American Giant Observatory<sup>1</sup>(LAGO) is an extended CR observatory composed of a network of WCDs spanning over different sites located at significantly different altitudes and extended from Mexico to Antarctica. Currently, LAGO has three main scientific objectives: to study high energy gamma events at high altitude sites, to understand space weather phenomena and monitoring it at continental scale and decipher the impact of the cosmic radiation on atmospheric phenomena [3]. WCDs exhibit a rather uniform exposure up to large zenithal angles and are sensitive to charged particles as well as to energetic photons which convert to pairs in the water volume. Furthermore, WCDs are robust, they have low cost and last but not least, easy maintenance and eco-friendly. In this work we present the first two-year observations of a new WCD installed for space weather studies in 2019 at the Argentinean Marambio station in the Antarctic Peninsula, being the southernmost detector of LAGO Observatory. Secondary cosmic rays (SCRs) flux generated as a result of interactions of primary cosmic ray particles with air nuclei in the atmosphere, present variations due to atmospheric effects as pressure and temperature profile changes. Thus, for the study of variations associated with interplanetary processes it is necessary to make corrections due to meteorological effects. This work is organized as follows: in Section 2 the LAMP Group and the Antarctic SW laboratory are presented, in Section 3 the detector, the data acquisition system (DAQ) and the energy calibration are described. Then, in Section 4, the performed observations are shown, the barometric effect is removed and a comparison with Oulu Neutron Monitor is done. Finally, in Section 5 the conclusions and future perspectives are presented.

## 2. LAMP Group & Antarctic SW laboratory

LAMP (acronym from spanish “Laboratorio Argentino de Metorología del esPacio”) is an inter-institutional (DCAO-FCEN-UBA, IAFE-UBA- CONICET and IAA-DNA) and inter-disciplinary group from Buenos Aires, Argentina, mainly dedicated to SW research, instrumental development,

---

<sup>1</sup><http://lagoproject.net/>

research-to-operations (R2O) and real-time monitoring of SW conditions<sup>2</sup> [4]. LAMP is full member of ISES (International Space Environment Service), and officially appointed as the Argentine Regional Warning Center (RWC). A project to install a SW laboratory at the Argentine Marambio Base in Antarctica (64.24S-56.62W, 196 m a.s.l., vertical geomagnetic rigidity cut-off: 2.32 GV [5]) was developed almost a decade ago [6]. Among the main scientific aims of the Antarctic SW laboratory can be found: (1) the study of astroparticles as tracers of SW in an interdisciplinary approach (2) analysis of the modulation of CRs from solar and magnetosphere conditions and (3) studies of particle cascades at ground and flight level and connections with atmospheric physics [7]. The construction of the laboratory and deployment of its instruments was done during the last three argentinean antarctic campaigns during the southern hemispheric summers of 2017/2018, 2018/2019 and 2019/2020. The main instrument installed was a WCD named Neurus, which is part of the LAGO detection network. The laboratory also has a magnetometer prototype, a GPS system to make the time stamp of observations, a meteorological station and a telemetry system which provides 5-minutes real-time monitoring at the servers of the group at Buenos Aires. Details of the WCD and the DAQ system are described in the next section.

### 3. Neurus WCD & DAQ system

Neurus WCD consists of a stainless steel cylindrical tank (diameter = 0.96 m, height = 1.20 m) which is full of purified water. When charged particles enter the detector with a speed greater than the speed of light in water, they produce Cherenkov radiation which is detected by a photomultiplier tube (PMT). An internal coating made from Tyvek® assures the reflection and diffusion of the Cherenkov photons inside the tank. It is known that WCDs enable the possibility of measure the muonic ( $\mu \pm$ ) and electromagnetic components ( $e \pm$  and  $\gamma$ ) of the extensive air showers (EAS) (e.g. [1]).

- Three DAQ systems were implemented:
- \* An oscilloscope in rate mode counts the pulses that exceed a peak threshold and then this rate is recorded by a communication system. The threshold was chosen in such a way as to include in the counts SCRs with deposited energy associated with the electromagnetic component.
  - \* A commercial board STEMLab Red Pitaya working as oscilloscope records the trace of five sample pulses per second, limited by the acquisition speed of Red Pitaya in this mode and its communication with the computer.
  - \* The new data acquisition system of the LAGO Collaboration based on the Red Pitaya board which record the trace of all pulses detected.

#### 3.1 Energy calibration: Peak & Charge histograms

In this section we consider the 12329153 voltage pulses acquired by using the Red Pitaya in oscilloscope mode during April 2019 in order to show how the energy calibration is done. Figure 1 shows the peak histogram (left) and the charge histogram (right). The value of the maximum observed in the peak histogram is determined by the trigger threshold (0.02 V). The area of each voltage pulse  $V(t)$  is proportional to the energy deposited by the detected particles. The first peak is

<sup>2</sup><http://spaceweather.at.fcen.uba.ar/2/>

related to the chosen trigger threshold and is mainly generated by the electromagnetic component of the SCRs. Higher values of charge in the histogram correspond to simultaneous entrance of multiple particles to the detector called mini-showers. Intermediate values, evidenced by a characteristic peak called the muon hump, are dominated by single muons crossing the detector. Deposited energy by muons with vertical incidence is proportional to its track length in water. Since a muon in water deposits  $2 \text{ MeV cm}^{-1}$  of energy and considering the water level in the tank is  $h = 100 \text{ cm}$ , it is possible to assign an energy value of 200 MeV to the energy deposited by the particles whose trace are pulses with areas equal to the second maximum of the histogram, and thus calibrate the histogram in units of Vertical-Equivalent Muon [VEM].

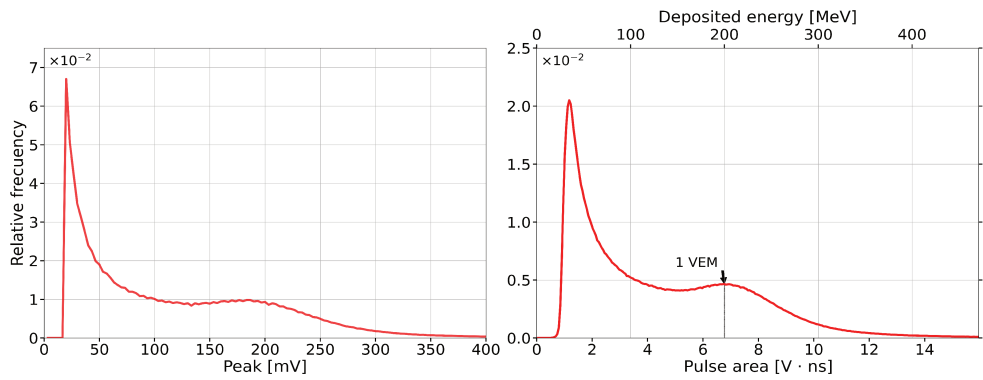


**Figure 1:** Peak (left) and pulse area (right) histograms for April 2019. The right panel also shows energy scale calibrated from VEM.

Since with this mode we are not recording all pulses, several days of data are needed to get these histograms with a good statistical. However, by considering the pulse area histograms acquired with the new LAGO DAQ system, which record all pulses, it is possible to get a count rate related to the flux of secondary particles in a specific range of deposited energy with an one-minute resolution [8].

#### 4. Data analysis

Since the installation of the detector in March 2019 some updates and improvements were made in the experiment. The entire observation period (March 2019 - June 2021) is divided into four sub-periods to highlight and summarize DAQ systems and improvements made in each one.

\* First: From 25th March 2019 to 31th December 2019. Two of the systems described in the previous section worked during this period: Oscilloscope and STEMlab Red Pitaya as oscilloscope. There was not laboratory room temperature control.

\* Second: From 1st January to 25 March, 2020 (2020 Antarctic campaign). The acquisition was stopped to carry out the updates.

\* Third: From 25 March 2020 to 31th December 2020. The new data acquisition system of the LAGO Collaboration based on the RedPitaya board was installed. Red Pitaya as oscilloscope didn't work for most of the period. A laboratory room temperature control system was installed.

\* Fourth: From January 2021 until now. The second update was carried out during the 2021 Antarctic campaign without stopping the acquisition. All the described modes have been operational since then.

We build the hourly-average count rate ( $S$ ), the surface pressure measurement ( $P$ ) and internal temperature ( $T$ ) for the four periods (see Figure 2). In this work we analyze the data of the first and the third period. The count rate  $S$  is acquired by the oscilloscope, which is the only DAQ system that have been working since the detector began its observations. Its average is around 160 counts per second. In the next section we analyze the atmospheric effects on  $S$ .

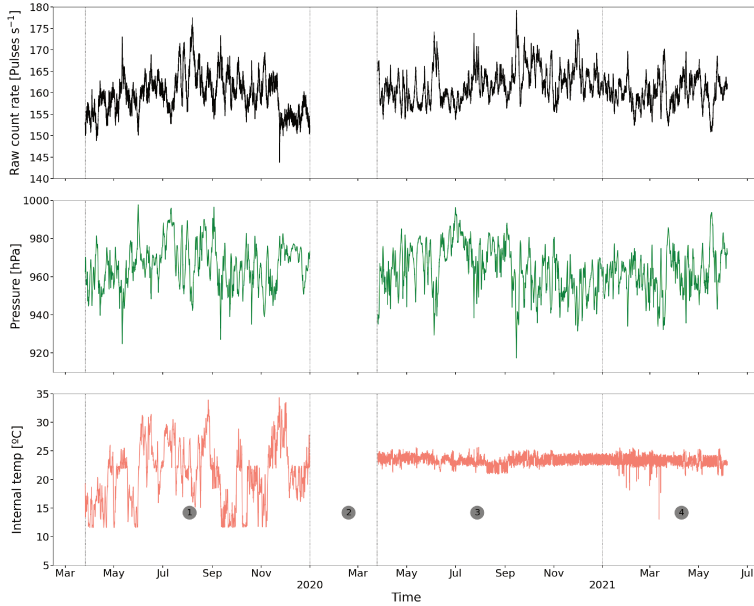


**Figure 2:** Hourly-average raw count rate ( $S$ ), surface atmospheric pressure measurement ( $P$ ) and laboratory room temperature ( $T$ ) for the whole observation period.

#### 4.1 Barometric effect

To analyze the barometric effect for periods 1 and 3, we consider time intervals of one month. We decide to keep months in which the surface pressure varied by at least 25 hPa and the Pearson correlation coefficient between  $S$  and  $P$  is higher than 0.9. The selected months are: May, July and August of 2019 and May, June, July and September of 2020. In such a way, most of the variability of these months is associated only with pressure effects and not with others sources as temperature variations, geomagnetic or interplanetary effects. As a first approach, we assume a linear relation between  $S$  and  $P$ :

$$\frac{\Delta S}{S_0} \times 100\% = \beta \Delta P \quad (1)$$

where  $\Delta S = S - S_0$  and  $\Delta P = P - P_0$ ,  $S_0$  and  $P_0$  are the mean count rate and pressure, respectively, of the time period considered. The barometric coefficient  $\beta$  depends on many factors, such as the nature and energy of the secondary particles and the altitude of the observation place.

For each selected month we have performed a linear fit based on Equation 1. As an example, we show in Figure 3 the the linear regression for July 2019 and 2020, which is the month with the highest Pearson's coefficient in both years. Finally, we measure  $\beta$  making the mean of the slopes obtained in each of these months and we obtain  $\beta = -(0.20 \pm 0.03) \text{ \% hPa}^{-1}$ .

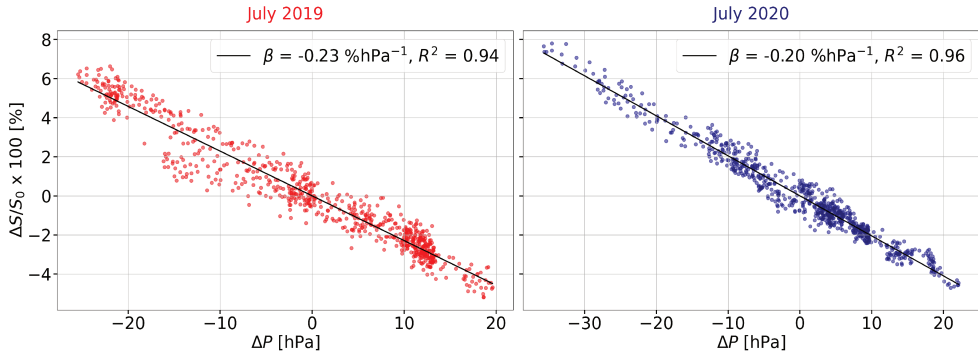


**Figure 3:**  $\frac{\Delta S'}{S'_0} \times 100\%$  vs.  $\Delta P$  and regression lines for July 2019 (left) and July 2020 (right).

We use this  $\beta$  to remove the pressure effect in the full ranges of period 1 and 3. Figure 4 shows the time series of the pressure-corrected count rate  $\frac{\Delta S'}{S'_0} \times 100\%$  for 2019 (left panel) and 2020 (right panel). A seasonal modulation with a maximum in winter and a minimum in summer can be observed in both periods, with a higher amplitude during 2019 which at first could be influenced by the intenal temperature. Seasonal effect in low-energy muon flux due to changes of atmospheric temperature profile is discussed in several works [9] and it will be considered in the near future to evaluate an adequate correction of this atmospheric effect.

#### 4.2 Comparison with Oulu Neutron Monitor

We make a comparison between Marambio WCD and a neutron monitor. We select Oulu NM because its long-term stability and its vertical geomagnetic rigidity cut-off, which is similar and a bit lower than the one at Marambio, about 0.8 GV. Oulu NM is located at 65.05N – 25.47E and 15 m a.s.l. We consider the pressure-corrected count rate with an hour base for both observatories and

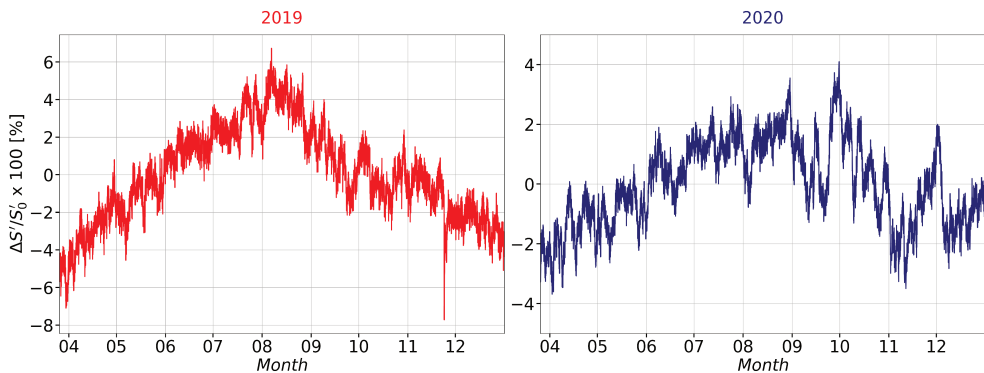


**Figure 4:** Time series of pressure-corrected count rate for 2019 (left) and 2020 (right).

calculate the Spearman's correlation coefficient  $r_s$  between the two standarized series (null mean and standard deviation equal to one) for each month of period 1 and 3. We also remove the trend observed in each month due to the seasonal effect in the WCD data. We expect that months with the highest association will be those in which the variability due to the local atmospheric effects of Marambio is not significant and, therefore, most of the variability is related to the flux of primary particles. In Figure 5 we show the comparison for April 2019 ( $r_s = 0.20$ ) and December 2020 ( $r_s = 0.55$ ), which are the months with the highest Spearman's correlation for period 1 and 3, respectively.

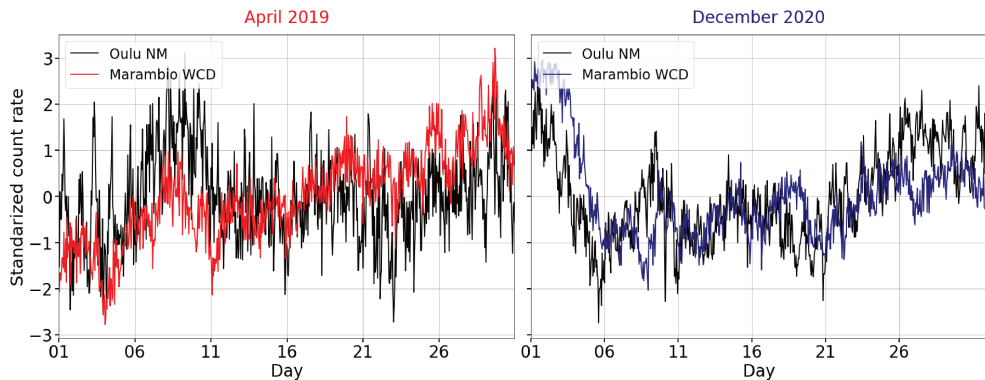


**Figure 5:** Comparison between pressure-corrected count rate of Neurus WCD and Oulu NM for April 2019 (left) and December 2020 (right). These months presented the highest Spearman's correlation in 2019 and 2020, respectively.

This comparison is a way of validating our observations. However, not in all periods we find a good correlation. Due the two particle monitors measure different types of particle it is necessary to improve the comparison.

## 5. Conclusion

In this work we have presented a new CR detector for space weather studies based on Water Cherenkov effect, installed in the Antarctic Peninsula in 2019, as part of the LAGO project. We have shown observations made during the first two years of operation. From these data we have estimated the barometric coefficient  $\beta$  from the data, obtaining  $\beta = -(0.20 \pm 0.03) \% \text{ hPa}^{-1}$ . After removing the barometric effect using  $\beta$ , a seasonal effect was observed. In the first year the laboratory room temperature was not controlled, while in the other years it was in an optimal range between 24 and 22 °C. In addition we compared our observations with the ones from Oulu NM, which results in good agreement in determined months. To make progress in the calibration of the detector, in the near future we will study the effect of the vertical temperature profile, in order to identify variability associated with interplanetary effects. On the other hand, we can calibrate our detector in energy using charge histograms and from knowing the energy deposited by a vertical muon. Since 2020, we obtained a high-statistics charge histogram every minute. This will allow us to build the count rate for different type of particles and study the atmospheric effects in each one, in future works.

## Acknowledgments

The authors acknowledge support from the Argentinean grants UBACYT (UBA) and PICT-2019-02754 (FONCyT-ANPCyT). LAGO collaboration is very grateful to all the participating institutions and The Pierre Auger collaboration for their continuous support. Acknowledgements to the NMDB database, founded under the European Union's FP7 programme for providing data, as well as to the Oulu neutron monitor webpage and the Sodankyla Geophysical Observatory.

## References

- [1] Pierre Auger Collaboration, P. Abreu, M. Aglietta, E.J. Ahn, D. Allard, I. Allekotte et al., *The Pierre Auger Observatory scaler mode for the study of solar activity modulation of galactic cosmic rays*, *Journal of Instrumentation* **6** (2011) 1003.
- [2] S. Dasso, H. Asorey and Pierre Auger Collaboration, *The scaler mode in the Pierre Auger Observatory to study heliospheric modulation of cosmic rays*, *Advances in Space Research* **49** (2012) 1563 [[1204.6196](#)].
- [3] I. Sidelnik, H. Asorey and LAGO Collaboration, *LAGO: The Latin American giant observatory*, *Nuclear Instruments and Methods in Physics Research A* **876** (2017) 173 [[1703.05337](#)].
- [4] V. Lanabere, S. Dasso, A.M. Gulisano, V.E. López and A.E. Niemelä-Celeda, *Space weather service activities and initiatives at LAMP (Argentinean Space Weather Laboratory group)*, *Advances in Space Research* **65** (2020) 2223.
- [5] S. Masias-Meza, J. & Dasso, *Geomagnetic effects on cosmic ray propagation under different conditions for Buenos Aires and Marambio, Argentina*, *Sun and Geosphere* **9** (2014) 41 [[1402.6274](#)].
- [6] S. Dasso, A.M. Gulisano, J.J. Masías-Meza and H. Asorey, *A Project to Install Water-Cherenkov Detectors in the Antarctic Peninsula as part of the LAGO Detection Network*, *PoS ICRC2015* (2016) 105.
- [7] A. Gulisano, S. Dasso, O. Areso, M. Pereira, N. Santos, L.V. Lopez, Viviana et al., *State of the art and challenges of the Argentine space weather laboratory (LAMP) in the Antarctic Peninsula*, *Boletín de la Asociación Argentina de Astronomía* (2021, In press).
- [8] M.S. Durán, H. Asorey, S. Dasso, L. Nunez, Y. Pérez and C. Sarmiento, *The LAGO Space Weather Program: Directional Geomagnetic Effects, Background Fluence Calculations and Multi-Spectral Data Anal*, *PoS ICRC2015* (2016) 142.
- [9] R.R.S. de Mendonça, J.P. Raulin, E. Echer, V.S. Makhmutov and G. Fernandez, *Analysis of atmospheric pressure and temperature effects on cosmic ray measurements*, *Journal of Geophysical Research (Space Physics)* **118** (2013) 1403.

## Full Authors List: LAGO Collaboration

V. Agosín<sup>17</sup>, A. Alberto<sup>3</sup>, C. Alvarez<sup>16</sup>, J. Araya<sup>20</sup>, R. Arceo<sup>16</sup>, O. Areso<sup>13</sup>, L. H. Arnaldi<sup>32</sup>, H. Asorey<sup>14,7</sup>, M. Audelo<sup>9</sup>, M.G. Ballina-Escobar<sup>19</sup>, D.C. Becerra-Villamizar<sup>18</sup>, X. Bertou<sup>2</sup>, K.S. Caballero-Mora<sup>16</sup>, R. Caiza<sup>8</sup>, R. Calderón-Ardila<sup>14</sup>, J. Calle<sup>24</sup>, A. C. Fauth<sup>27</sup>, E. Carrera Jarrin<sup>26</sup>, L. E. Castillo Delacroix<sup>11</sup>, C. Castromonte<sup>25</sup>, D. Cazar-Ramírez<sup>26</sup>, D. Cogollo<sup>28</sup>, D.A. Coloma Borja<sup>26</sup>, R. Conde<sup>1</sup>, J. Cotzomi<sup>1</sup>, D. Dallara<sup>11</sup>, S. Dasso<sup>13,5,6</sup>, R. Aguiar<sup>27</sup>, A. Albuquerque<sup>28</sup>, J.H.A.P. Reis<sup>27</sup>, H. De León<sup>16</sup>, R. de León-Barrios<sup>23</sup>, D. Domínguez<sup>8</sup>, M. Echiburu<sup>21</sup>, M. González<sup>2</sup>, M. Gómez Berisso<sup>2</sup>, J. Grisales Casadiegos<sup>23</sup>, A. M. Gulisano<sup>13,12,6</sup>, J.C. Helo<sup>17</sup>, C.A.H. Condori<sup>24</sup>, J. E. Ise<sup>11</sup>, G. K. M Nascimento<sup>28</sup>, M. A. Leigui de Oliveira<sup>29</sup>, F. L. Miletto<sup>27</sup>, V. P. Luzio<sup>29</sup>, F. Machado<sup>25</sup>, J.F. Mancilla-Caceres<sup>22</sup>, D. Manriquez<sup>20</sup>, A. Martínez-Méndez<sup>23</sup>, O. Martinez<sup>1</sup>, R. Mayo-García<sup>3</sup>, L.G. Mijangos<sup>22</sup>, P. Miranda<sup>24</sup>, M. G. Molina<sup>11</sup>, I.R. Morales<sup>19</sup>, O.G. Morales-Olivares<sup>16</sup>, E. Moreno-Barbosa<sup>1</sup>, P. Muñoz<sup>17</sup>, C. Nina<sup>24</sup>, L.A. Núñez<sup>23</sup>, L. Otinianino<sup>4</sup>, R. Pagán-Muñoz<sup>3</sup>, K.M. Parada-Jaime<sup>18</sup>, H.M. Parada-Villamizar<sup>18</sup>, R. Parra<sup>10</sup>, J. Peña-Rodríguez<sup>23</sup>, M. Pereira<sup>13</sup>, Y.A. Perez-Cuevas<sup>18</sup>, H. Perez<sup>19</sup>, J. Pisco-Guabave<sup>23</sup>, M. Raljevic<sup>24</sup>, M. Ramelli<sup>13</sup>, C. Ramírez<sup>22</sup>, H. Rivera<sup>24</sup>, L. T. Rubinstein<sup>13,33</sup>, A.J. Rubio-Montero<sup>3</sup>, J.R. Sacahui<sup>19</sup>, H. Salazar<sup>1</sup>, N. Salomón<sup>11</sup>, J. Samanes<sup>4</sup>, N.A. Santos<sup>5</sup>, C. Sarmiento-Cano<sup>14</sup>, I. Sidelnik<sup>2</sup>, M.B. Silva<sup>22</sup>, O. Soto<sup>17</sup>, M. Suárez-Durán<sup>18,31</sup>, M. Subieta Vasquez<sup>24</sup>, C. Terrazas<sup>24</sup>, R. Ticona<sup>24</sup>, T. Torres Peralta<sup>11</sup>, P.A. Ulloa<sup>17</sup>, Z.R. Urrutia<sup>22</sup>, N. Vásquez<sup>8</sup>, A. Vázquez-Ramírez<sup>23</sup>, A. Vega<sup>20</sup>, P. Vega<sup>17</sup>, J. Vega<sup>4</sup>, A. Vesga-Ramirez<sup>14,34</sup>, D. Vitoreti<sup>30</sup>, R. Wiklich Sobrinho<sup>29</sup>

<sup>1</sup>Benemérita Universidad Autónoma de Puebla.<sup>2</sup>Centro Atómico Bariloche (CNEA/CONICET/IB).<sup>3</sup>CIEMAT.<sup>4</sup>Comisión Nacional de Investigación y Desarrollo Aeroespacial.<sup>5</sup>Departamento de Ciencias de la Atmósfera y los Océanos, DCAO (FCEN-UBA).<sup>6</sup>Departamento de Física, DF (FCEN-UBA).<sup>7</sup>Departamento Física Médica, CNEA-CONICET-UNSAM.<sup>8</sup>Escuela Politécnica Nacional.<sup>9</sup>Escuela Superior Politécnica de Chimborazo.<sup>10</sup>European Soutern Observatory (ESO).<sup>11</sup>Facultad de Ciencias Exactas y Tecnología (FACET) – Universidad Nacional de Tucumán (UNT) / CONICET.<sup>12</sup>Instituto Antártico Argentino, Dirección Nacional del Antartico.<sup>13</sup>Instituto de Astronomía y Física del Espacio, IAFE (UBA-CONICET).<sup>14</sup>Instituto de Tecnologías en Detección y Astropartículas (CNEA, CONICET, UNSAM).<sup>16</sup>Universidad Autónoma de Chiapas.<sup>17</sup>Universidad de La Serena.<sup>18</sup>Universidad de Pamplona.<sup>19</sup>Universidad de San Carlos.<sup>20</sup>Universidad de Valparaíso.<sup>21</sup>Universidad de Viña del Mar.<sup>22</sup>Universidad del Valle de Guatemala.<sup>23</sup>Universidad Industrial de Santander.<sup>24</sup>Universidad Mayor de San Andrés.<sup>25</sup>Universidad Nacional de Ingeniería.<sup>26</sup>Universidad San Francisco de Quito.<sup>27</sup>Universidade Estadual de Campinas (UNICAMP).<sup>28</sup>Universidade Federal de Campina Grande.<sup>29</sup>Universidade Federal do ABC.<sup>30</sup>Universidade Federal do Recôncavo da Bahia.<sup>31</sup>Université Libre de Bruxelles, Brussels, Belgium.<sup>32</sup>Centro Atómico Bariloche (CNEA/IB).<sup>33</sup>Laboratorio de Acústica y Electroacústica, LACEAC (FI-UBA).<sup>34</sup>International Center for Earth Sciences (CNEA, CONICET).